Zonal mean atmospheric distribution of sulphur hexafluoride (SF_6)

A. B. Burgess,[1] R. G. Grainger,[1] and A. Dudhia[1]

Received 6 December 2005; revised 14 February 2006; accepted 24 February 2006; published 8 April 2006.

[1] MIPAS is a polar orbiting high resolution mid-infrared limb emission sounder with a nominal vertical resolution of 3 km. Building on previous work, we determine global (90°N–90°S, 5° resolution) zonal mean distributions for sulphur hexafluoride from measurements between 6 and 36 km. The time evolution of the global structure is useful for age of air determination and the validation of dynamics in atmospheric models. By comparing solstice and equinox months from 2002 through to 2004, we observe differences which shift with seasonal changes in atmospheric circulation. In addition, a clear systematic increase in the SF_6 loading with time is observed globally (0.30 ± 0.025 pptv yr^{-1}). This is compared against independent surface measurements.
Citation: Burgess, A. B., R. G. Grainger, and A. Dudhia (2006), Zonal mean atmospheric distribution of sulphur hexafluoride (SF_6), *Geophys. Res. Lett.*, *33*, L07809, doi:10.1029/2005GL025410.

1. Introduction

[2] Sulphur hexafluoride (SF_6) is one of the most efficient greenhouse gases: a thousand times stronger than an equivalent volume mixing ratio (VMR) of CO_2 [*Ko et al.*, 1993]. However, the radiative forcing from SF_6 is small because its current atmospheric concentration is around five parts per trillion by volume (pptv) [*Thompson et al.*, 2004].

[3] The sources of SF_6 are almost entirely anthropogenic leakage [*Ko et al.*, 1993] and the atmospheric lifetime is of the order of several thousand years [*Patra et al.*, 1997]. It is inert in the troposphere and stratosphere, with its sink being photolysis and high energy electron capture in the mesosphere [*Reddmann et al.*, 2001]. As a consequence, the atmospheric concentration of SF_6 is consistently increasing by 0.2–0.3 pptv (5–8%) yr^{-1} [*Maiss et al.*, 1996; *Geller et al.*, 1997; *Burgess et al.*, 2004; *Thompson et al.*, 2004]. Due to this, SF_6 is ideal as a long-term tracer of atmospheric motion and for calculating the age of stratospheric air.

[4] The Michelson Interferometer for Passive Atmospheric Sounding (MIPAS) was launched into a polar orbit as part of Europe's ENVISAT project. MIPAS is an actively cooled atmospheric thermal emission limb sounder, working in the mid-infrared with a field-of-view that is approximately 3 × 30 km. MIPAS obtains high resolution spectra (0.025 cm^{-1}) that cover the range 685–2410 cm^{-1} (14.6–4.15 μm). A nominal limb sequence consists of 17 spectra with tangent points at 68, 60, 52, 47, 42 and downward to 6 km in 3 km steps [*ESA*, 2000].

[5] In this paper, we describe the retrieval of SF_6 profiles using a space-based instrument and the coaddition of these profiles to form zonal mean fields. We then use these results to establish the global trend and seasonal changes in its distribution.

2. Retrieval

[6] The SF_6 signal exceeds the MIPAS noise-equivalent spectral radiance (NESR) between 944 and 951 cm^{-1}, corresponding to its main infrared vibrational-rotational transition region; centred around a single ν_3 Q branch at 947.9 cm^{-1}.

[7] Our retrieval has been performed with the 'MORSE' software [*Dudhia*, 2005] using the optimal estimation method [*Rodgers*, 2000]. This finds the most probable solution consistent with the measurements and a priori knowledge. Our approach makes use of microwindows [*Dudhia et al.*, 2002], which are small regions of the spectrum covering the majority of the SF_6 emission range.

[8] Figure 1 shows the averaging kernels for a single idealised profile. The vertical width is a measure of retrieval resolution and the area indicates the fraction of the retrieval that comes from the measurements as opposed to the a priori. Study of the averaging kernels allows us to determine which levels provide the most information.

[9] The general approach, microwindow selection, error analysis and initial validation used in the retrieval of SF_6 profiles from MIPAS data has been discussed previously in [*Burgess et al.*, 2004]. A trend of $+0.28 \pm 0.06$ pptv yr^{-1} was also determined.

2.1. Errors

[10] The microwindow selection process models the propagation of random and systematic errors through the retrieval, providing a full error analysis. It also allows the minimisation of many systematic errors by masking out individual spectral points. As a result, the whole spectral interval may be used. In addition, it results in a list of interfering species, ordered by significance. The most dominant, water, was jointly retrieved with pT and SF_6. Marginal interferences (O_3, N_2O, NO_2, HNO_3, NH_3, COF_2) were modelled using seasonally-adjusted climatologies during the retrieval. However, several 'model parameter errors' [*Rodgers*, 2000] remain.

[11] One of the most problematic lies in a persistent oscillation in the retrieved profiles around the tropical tropopause that is present in up to 30% of the retrievals. This effect can be recreated by simulating certain equatorial atmospheres on a fine vertical grid, where the temperature structure is unresolved by the 3 km instrument field of view. Due to this simulation result, it is justifiable to remove the oscillating profiles from further consideration.

[12] A second, systematic, error lies in the HITRAN-derived spectroscopic database [*Flaud et al.*, 2003] used in

[1]Atmospheric, Oceanic and Planetary Physics, Clarendon Laboratory, University of Oxford, Oxford, UK.

0094-8276/06/2005GL025410$05.00

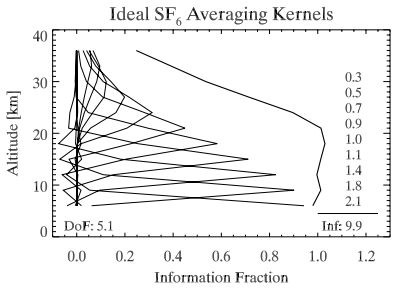

Figure 1. Ideal case averaging kernels for nominal noise values and retrieval over 9 levels. There are just over 5 degrees of freedom in this profile. The Shannon information gain for this retrieval was 9.9 bits with individual level contributions shown. There is significant prior information contribution above 25 km although it does not reach 50% until 30 km.

both the microwindow selection and the forward model segment of the retrieval. For SF_6, the temperature dependant cross-section data is the same as in HITRAN. It has been estimated that there is a 3–6% error on the SF_6 measurements used [*Flaud*, 2003]. This error should have a purely multiplicative scaling effect on the retrieved values.

[13] Finally, there is a bias at high altitude caused by the influence of the priori information on the result, discussed below.

2.2. Coaddition

[14] To generate the zonal means, gridding and subsequent coaddition of the profiles is required. When calculating means of retrieved profiles, the contribution of a priori information into the final result must be taken into account.

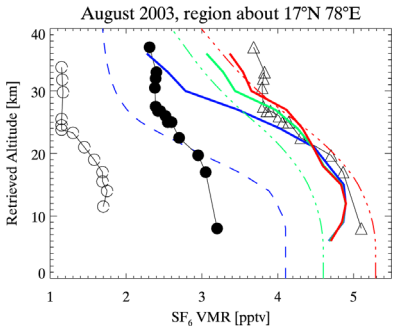

Figure 2. The result of combining approximately 1,000 MIPAS profiles, centred about 17°N, 78°E. Literature balloon values at the same location [*Patra et al.*, 1997] from 1987 (open circles) and 1994 (solid circles) are shown. The 1994 profile has been uniformly scaled to match the magnitude of the mean 2003 MIPAS profile by 2.2 pptv (0.25 pptv yr^{-1}, open triangles). The heavy blue line shows the MIPAS result, with the dashed blue line representing the a priori. The effect of removing the prior information and replacing it with two estimated a posteriori values (coloured dot-dash lines) is also shown. The latter estimate (red) was chosen to minimise the difference between retrieval and a priori for the high altitudes. The choice of a priori has little effect below 25 km, where the information from the measurements is dominant.

As we obtain a full covariance ($\mathbf{S}_{\hat{\mathbf{x}}}$) for each retrieval ($\hat{\mathbf{x}}$) it is possible to make use of the following relation [*Rodgers*, 2000] to determine an improved profile estimate:

$$\hat{\mathbf{x}}' = \left(\mathbf{S}_{\hat{\mathbf{x}}}^{-1} - \mathbf{S}_a^{-1} + \mathbf{S}_b^{-1}\right)^{-1}\left[\mathbf{S}_{\hat{\mathbf{x}}}^{-1}\hat{\mathbf{x}} - \mathbf{S}_a^{-1}\mathbf{x}_a + \mathbf{S}_b^{-1}\mathbf{x}_b\right] \quad (1)$$

where $\mathbf{x}_a$ is the a priori used for the retrieval, $\mathbf{x}_b$ is an optimised profile determined a posteriori and $\mathbf{S}_a = \mathbf{S}_b$. All covariances are were appropriately weighted considering the number of elements in the mean. The substitution approach is better than the simple removal of the a priori by $\hat{\mathbf{x}}'' = (\mathbf{S}_{\hat{\mathbf{x}}}^{-1} - \mathbf{S}_a^{-1})^{-1}[\mathbf{S}_{\hat{\mathbf{x}}}^{-1}\hat{\mathbf{x}} - \mathbf{S}_a^{-1}\mathbf{x}_a]$, because $\mathbf{S}_{\hat{\mathbf{x}}}^{-1} - \mathbf{S}_a^{-1}$ will be singular if the problem is under-constrained – common when the random noise is dominant in a set of measurements.

3. Results

[15] Observed vertical profiles of SF_6 from balloon [*Patra et al.*, 1997] are shown alongside MIPAS measurements from a similar geolocation in Figure 2. The influence of prior information at high altitude can also be seen, along with the effect of its correction. A single estimated a posteriori $\mathbf{x}_b$ was estimated after retrieval and was used globally, which prevents the introduction of prior latitudinal structure, but has the effect of reducing the vertical dynamic range of the retrieval. It was applied after the calculation of the mean profile in each case.

3.1. Zonal Means

[16] The zonal means were calculated by binning all successful cloud free retrieved profiles to 5° latitude bands. The mean profile was then taken and the a posteriori correction applied. Each month yielded 5–10,000 profiles overall, giving several hundred profiles per latitude band. The zonal mean for September 2003 is shown in Figure 3.

[17] Zonal mean differences from an annual mean field for equinox and solstice months are shown in Figure 4. There are clear tropospheric and stratospheric regions. The decrease in VMR with altitude is due almost entirely to the increasing age of the air at higher altitudes, as there is no significant loss mechanism for SF_6 in the troposphere and stratosphere.

[18] The equatorial troposphere region is screened out due to significant cloud effects bringing the number of

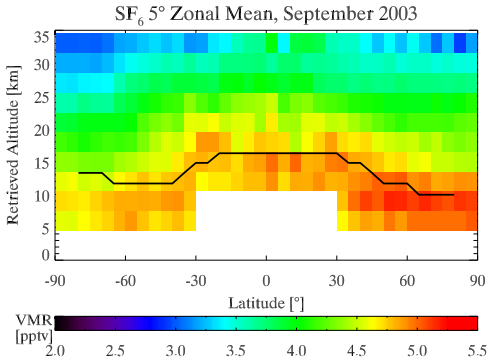

Figure 3. Zonal mean for September 2003. A climatological tropopause is indicated by the dark line. Low values over the South pole are assigned to wintertime mesospheric descent.

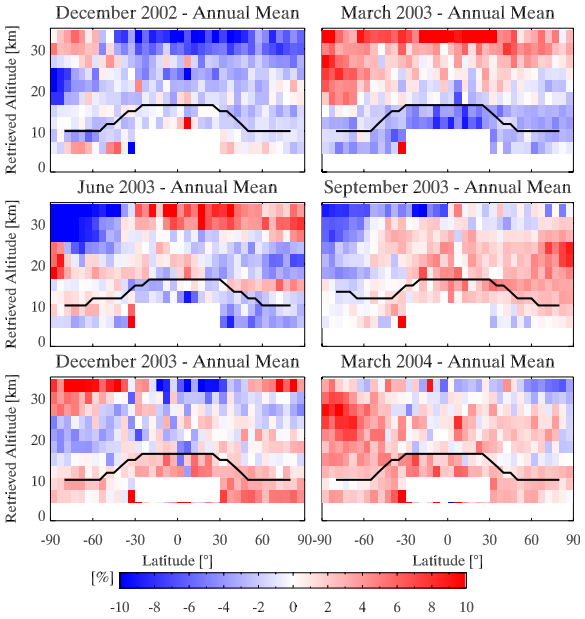

Figure 4. Zonal means for equinox and solstice months, December 2002 to March 2004. These allow the investigation of interannual variability (consistency of gross features) and seasonal trends (month-to-month variability).

successful retrievals down to a few tens of profiles and introducing some retrieval instabilities.

[19] The main features are dynamical – the change in the tropical tropopause 'centre', which is only centred over the equator for the equinoxes, and the descent of polar air. Some finer structure may also be resolved, such as the transport of tropospheric air into the stratosphere either side of the tropical tropopause, although the statistical significance of the measurements makes a firm conclusion difficult. There is also the year-on-year increase in the amount of SF_6 in the atmosphere, as already discussed. Other features to note include the hemispheric VMR difference and the overall smoothness of the zonal field. Each profile in the mean was wholly independent of the others and the a priori contained no latitudinal structure. As a result, the features originate from the SF_6 retrieval. No corresponding persistent errors in the temperature or water fields have been found that would explain this latitudinal structure.

[20] The difference in hemispheric mean VMRs (0.1–0.2 pptv) is in line with an inter-hemispheric transport time of the order of one year [*Waugh and Hall*, 2002], based on geolocation of the sources of SF_6. It is absent in the stratosphere, which is in line with our understanding of atmospheric circulation and the entry of tropospheric air into the stratosphere through a well mixed region in the tropics. Prior work by [*Geller et al.*, 1997] gave an inter-hemispheric difference of 0.27 ± 0.02 pptv from fixed surface sampling.

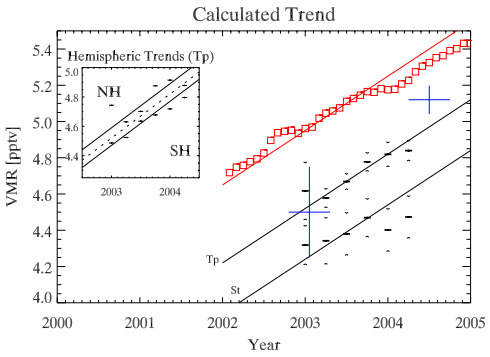

Figure 5. The trend in SF_6 VMR calculated from MIPAS measurements. The tropospheric (Tp) and stratospheric (St) global monthly means are shown along with best fit lines of 0.30 pptv yr^{-1}. Surface FTIR [*Rinsland et al.*, 2003] and satellite [*Rinsland et al.*, 2005] measurements are shown (large crosses). Monthly mean surface flask measurements (mean precision 0.09 pptv) from GMD/CATS are shown as squares, with the same trend line. The MIPAS data shows an almost constant offset that may be partially assigned to the 3–6% SF_6 spectroscopic error discussed earlier. This does not influence the calculated trend. The finer structure in the CATS data may be observed in the MIPAS measurements, where both show corresponding wintertime 'plateau' regions. The inset shows the hemispheric variability of MIPAS measured SF_6, about 0.12 pptv.

3.2. Trends in VMR

[21] We looked at measurements up to 15 months apart, expecting an increase of the order of 0.4 pptv corresponding to previous trend estimates. The observed variation within tropospheric values for a similar geolocation is approximately 0.5 pptv, and we assume that SF_6 is well mixed within the region. Hence the means of multiple orbits are required to reduce the random component to less than 0.05–0.01 pptv — enough to be certain of distinguishing a trend with statistical significance.

[22] The resultant mean tropospheric VMRs and calculated trend are shown in Figure 5, with remotely sensed data from the literature for comparison. The global and hemispheric means for the MIPAS data set are shown in Table 1. The standard deviations (SDs) of the tropospheric monthly mean values are all less than 0.25 pptv, which includes the effects of both random error on individual measurements as well as global variability. The hemispheric SDs are smaller than this. The uncertainty on the means, a function of the retrieval accuracy and the large number of measurements taken, is of the order 0.01 pptv in the stratosphere and 0.005 pptv in the troposphere.

[23] Considering the global mean tropospheric VMR for monthly sets of orbits, we find a global minimum value for March 2003 (4.58 ± 0.001 pptv) and a maximum for December 2003 (4.82 ± 0.002 pptv). A best fit linear regression of the six months sampled gives a trend of 0.30 ± 0.01 pptv yr^{-1} (Figure 5). The absolute mean values still contain the spectroscopic systematic bias already dis-

Table 1. Trends in Observed VMR

	Troposphere			Stratosphere		
Month VMR, pptv	NH	Global	SH	NH	Global	SH
December 2002	4.71	4.60	4.49	4.30	4.32	4.34
March 2003	4.63	4.58	4.52	4.32	4.35	4.38
June 2003	4.70	4.67	4.64	4.40	4.39	4.38
September 2003	4.88	4.78	4.68	4.52	4.48	4.45
December 2003	4.91	4.82	4.72	4.40	4.41	4.42
March 2004	4.90	4.84	4.79	4.44	4.47	4.50

cussed, but as the spectral database was constant for all months, the trend estimate is unchanged.

[24] Part of our observed trend was thought to be due to the influence of systematic errors that were changed by one of several MIPAS processor upgrades upstream of our retrieval process between September 2002 and October 2003. However, during 2005 a concerted effort has been made to ensure that all available L1B data is consistently radiometrically calibrated. Nevertheless, the main systematic error components expected to affect the trend are those related to instrument calibration which might remain correlated for months. Fortunately, the MW error analysis shows the dominant gain calibration error to be a minor effect. There is good reason to believe that the resultant influence on the retrievals has been small, based on the observed consistency of MIPAS operational products routinely analysed at Oxford from July 2002. For example, the equivalent trend in retrieved methane (around 45°N) is <1% at 12 km over the same period. A long-term systematic error in the spectral radiances would be expected to perturb the retrievals of all species.

[25] These trend values are in line with the most recent data from surface flask measurements by the NOAA Global Monitoring Division (GMD) Chromatograph for Trace Species experiments (CATS) of 0.24 pptv yr^{-1} for 2004 [*Thompson et al.*, 2004]. Similarly, infrared spectroscopic measurements by [*Krieg et al.*, 2005] give trend values that range from $0.24-0.31 \pm 0.08$ pptv yr^{-1} for various surface sites. [*O'Connell et al.*, 2000] suggest that the rate of increase of emission has decreased over the last decade due to increased environmental awareness, so attempting to fit a single trend that encompasses historic measurements from the early 1990s as well as current results may not be useful for future loading prediction.

4. Conclusions

[26] SF_6 is at the borderline of detectability using the nominal retrieval methodology of one scan sequence to one profile. However, statistical treatments of the results have revealed underlying profiles that differ consistently from the assumed climatology. This deviation is in agreement with published trends, and is a useful piece of external validation and verification of the retrieval accuracy

[27] Data from MIPAS is able to provide regular global information on latitudinal VMRs and on their trends. We have demonstrated the feasibility of profile retrievals in the range 6–30 km based on single scans, with 4–5 degrees of freedom for each profile. Averaging of multiple orbits to reduce random errors has been successful. A mean mid-latitude profile shows distinct tropospheric — 4.78 ± 0.007pptv, global variability SD 0.17 pptv, September 2003 — and mass weighted stratospheric (4.48 ± 0.008 pptv, SD 0.81 pptv) regimes. This global mean stratospheric loading contains an inter-hemispheric variability of the order of 0.1–0.2 pptv, giving an inter-hemispheric exchange time (troposphere) of a little less than one year. Finally, we have shown the continuation of acknowledged global trends in atmospheric concentration, placing our estimate at 0.30 ± 0.01 pptv yr^{-1}.

[28] Future work would use the wealth of available MIPAS data for circulation model validation. It would also explore using MIPAS SF_6 as an inert tracer for calculating the age of stratospheric air as well as examining stratospheric descent, at a coarse time resolution. Possibilities also exist for combining SF_6 with other zonal MIPAS targets to determine an age spectrum.

[29] **Acknowledgment.** We would like to acknowledge NERC (UK) for providing funding, Geoff Dutton and others at GMD/CATS (www.cmdl.noaa.gov) for providing the SF_6 surface flask data and two very helpful anonymous reviewers.

References

Burgess, A., R. Grainger, A. Dudhia, V. Payne, and V. Jay (2004), MIPAS measurements of sulphur hexafluoride (SF_6), *Geophys. Res. Lett.*, *31*, L05112, doi:10.1029/2003GL019143.

Dudhia, A. (2005), The MIPAS Orbital Retrieval using Sequential Estimation (MORSE), technical report, Univ. of Oxford, Oxford, U.K. (available at www.atm.ox.ac.uk/MORSE)

Dudhia, A., V. Jay, and C. Rodgers (2002), Microwindow selection for high spectral resolution sounders, *Appl. Opt.*, *41*, 3665–3673.

European Space Agency (2000), ENVISAT MIPAS—An instrument for atmospheric chemistry and climate research, *Eur. Space Agency Spec. Publ.*, *ESA SP-1229*, 124 pp.

Flaud, J.-M. (2003), Review of spectroscopic parameters (WP1300), *ESA ITT AO/1-4232/02/I-LG*, 33 pp., Eur. Space Agency, Paris.

Flaud, J.-M., C. Piccolo, B. Carli, A. Perrin, L. C. Teffo, and L. Brown (2003), Molecular line parameters for the MIPAS experiment, *J. Atmos. Ocean Opt.*, *16*, 172–182.

Geller, L., J. Elkins, J. Lobert, A. Clarke, D. Hurst, J. Butler, and R. Myers (1997), Tropospheric SF_6: Observed latitudinal distribution and trends, derived emissions and interhemispheric exchange time, *Geophys. Res. Lett.*, *6*, 675–678.

Ko, M., N. D. Sze, W.-C. Wang, G. Shia, A. Goldman, F. Murcary, D. Murcary, and C. Rinsland (1993), Atmospheric sulfur hexafluoride: Sources, sinks and greenhouse warming, *J. Geophys. Res.*, *98*, 10,499–10,507.

Krieg, J., J. Nothholt, E. Mahieu, C. Rinsland, and R. Zander (2005), Sulphur hexafluoride (SF_6): Comparison of FTIR-measurements at three sites and determination of its trend in the Northern Hemisphere, *J. Quant. Spectrosc. Radiat. Transfer*, *92*, 383–392.

Maiss, M., L. Steele, R. Francey, P. Fraser, R. L. N. Trivett, and I. Levin (1996), Sulfur hexafluoride—A powerful new atmospheric tracer, *Atmos. Environ.*, *30*, 1621–1629.

O'Connell, P., F. Heil, J. Henriot, G. Mauthe, H. Morrison, L. Niemeyer, M. Pittroff, R. Probst, and J. Taillebois (2000), SF_6 in the electric industry, status 2000, paper presented at CIGRE Working Group 23.02, Int. Counc. on Large Electr. Syst., Paris.

Patra, P., S. Lal, B. Subbaraya, C. H. Jackman, and P. Rajaratnam (1997), Observed vertical profile of sulfur hexafluoride (SF_6) and its atmospheric applications, *J. Geophys. Res.*, *102*, 8855–8859.

Reddmann, T., R. Ruhnke, and W. Kouker (2001), Three-dimensional model simulations of SF_6 with mesospheric chemistry, *J. Geophys. Res.*, *106*, 14,525–14,537.

Rinsland, C., A. Goldman, T. Stephen, L. Chiou, E. Mahieu, and R. Zander (2003), SF_6 ground-based infrared solar absorption measurements: Long-term trend, pollution events, and a search for SF_5CF_3 absorption, *J. Quant. Spectrosc. Radiat. Transfer*, *78*, 41–53.

Rinsland, C., C. Boone, R. Nassar, K. Walker, P. Bernath, E. Mahieu, R. Zander, J. McConnell, and L. Chiou (2005), Trends of HF, HCl, CCl_2F_2, CCl_3F, $CHClF_2$ (HCFC-22), and SF_6 in the lower stratosphere from Atmospheric Chemistry Experiment ACE and Atmospheric Trace Molecule Spectroscopy ATMOS measurements near 30°N latitude, *Geophys. Res. Lett.*, *32*, L16S03, doi:10.1029/2005GL022415.

Rodgers, C. D. (2000), *Inverse Methods for Atmospheric Sounding: Theory and Practice*, *Atmos., Oceanic, Planet. Phys.*, World Sci., Hackensack, N. J.

Thompson, T. M., et al. (2004), Halocarbons and other atmospheric trace species, in *Climate Monitoring Diagnostics Laboratory Summary Report 27*, edited by R. C. Schnell, A.-M. Buggle, and R. M. Rosson, pp. 115–135, Earth Syst. Syst. Res. Lab., Boulder, Colo.

Waugh, D., and T. Hall (2002), Age of stratospheric air: Theory, observations, and models, *Rev. Geophys.*, *40*(4), 1010, doi:10.1029/2000RG000101.

A. B. Burgess, A. Dudhia, and R. G. Grainger, Atmospheric, Oceanic and Planetary Physics, Clarendon Laboratory, University of Oxford, Parks Road, Oxford OX1 3PU, UK. (burgess@atm.ox.ac.uk)